Iranian Journal of Chemical Engineering
Vol. 4, No. 1 (Winter), 2007, IAChE

Research note

Synthesis and Seeding Time Effect on the Performance of Nanostructure Sodalite Membranes

B. Bayati[1], A.A. Babaluo[1,2], P. Ahmadian Namini[1]*

1- Nanostructure Materials Research Center (NMRC), Sahand University of Technology, Tabriz, I.R.Iran
2- Research Center of Polymeric Materials, Sahand University of Technology, Tabriz, I.R. Iran.

Abstract

Secondary growth technique was successfully applied for the synthesis of nanostructure sodalite membranes with vacuum seeding on tubular α-Al_2O_3 supports. In the seeding process, a thin, uniform and continuous seeding layer was closely attached to the support external surface by the pressure difference between the two sides of the support wall. The final nanostructure sodalite top-layers were synthesized on the seeded support into a stainless steel autoclave with a Teflon holder. The effect of seeding time on the microstructure of the synthesized sodalite top-layers was investigated at four different levels 60, 120, 180 and 240 s. The synthesized membranes were characterized by XRD, SEM and mercury porosimetry. The obtained results showed that sodalite zeolite was synthesized on the membranes top-layers with uniform surfaces. But, the top-layers thickness increases by increasing the seeding time and tends to reach a plateau. Further increasing the seeding time causes dense top-layers to form. Also, the performance of the manufactured sodalite membranes was evaluated by permeations of single gases (H2 and N2) under different pressure differences at a temperature of 283K. It is found that the membrane permeance shows a maximum value at seeding time 180 s with a constant permselectivity (H2/N2) of about 2.5. The permeation results were confirmed by SEM micrographs which showed a thick and low-dense top-layer in the membranes manufactured with the seeding time of 180 s.

Keywords: *Synthesis, Nanostructure, Sodalite, Membrane, Seeding Time*

Introduction

Zeolites or crystalline aluminosilicates are widely used in separation and refinery industries as catalysts, adsorbents and ion exchangers due to their meso and microporous (nanoporous: <50nm) structures [1,2]. The significant catalytic activity and selectivity of zeolite materials are attributed to the large internal surface area, highly distributed active sites that are accessible through uniform nanopore size [3,4], high thermal resistance, chemical inertness and high mechanical strength [5,6].

Sodalite is one of the microporous crystalline zeolites which consist of a cubic array of β-cages [7]. Sodalites are microporous tectosilicates of the general composition as $8[AlSiO_4]_6(X)_2$, where X is a monovalent guest anion as chlorine in the mineral sodalite[9]. This kind of zeolite has a six-membered ring aperture [7]. The six-membered ring of Si_ O_ Si bonds has a pore

∗ Corresponding author: E-mail: a.babaluo@sut.ac.ir

width of 2.8 °A, which makes interesting materials for the separation of small gases like H_2 or He from various gas streams [8]. Therefore, due to the unique applications of hydrogen [9], the synthesis of sodalite membranes for hydrogen purification processes is very important.

Several preparation methods have been developed for sodalite membranes synthesis such as in situ hydrothermal synthesis[6], the vapor phase transport method, the microwave hydrothermal method, embedding micro-crystals of zeolite into a matrix [7], secondary growth technique [10], and etc. In this work, a new route was applied for the synthesis of sodalite zeolite seeds and sodalite membranes based on the α-Al_2O_3 tubular supports via a hydrothermal (secondary growth) technique. Also, due to the critical rule of the nucleation seeds [11] in the formation of thin and uniform zeolite membranes on the supports surface, the effect of seeding time on the microstructure, morphology and the performance of the manufactured sodalite membranes was investigated. Finally, we evaluated the performance of these membranes by the permeations of single gases (H_2 and N_2) under different pressure differences at a temperature of 283K and predicted an optimum time for seeding the sodalite zeolite seeds on the α-Al_2O_3 tubular supports.

Experimental

Material

The characteristics of material used in this work are given in Table 1 and Figure 1.

Table 1. Characteristics of materials

Materials	Function	Molecular formula	Characteristics	Supplier
α -Alumina	Ceramic phase (support)	α -Al_2O_3 See Fig. 1	average particle size: 1μm Powder	Fibrona[a]
Acrylamide (AM)	Monofunctional monomer	$C_2H_3CONH_2$	Molecular weight: 71.08 solid white	Merck[b]
N,*N*'-Methylene bis-acrylamide (MBAM)	Difunctional monomer (crosslinker)	$(C_2H_3CONH_2)_2CH_2$	Molecular weight: 154.2 solid white	Merck[b]
Ammonium persulfate	Initiator	$(NH_4)_2S_2O_8$	Molecular weight: 228.2 solid white powder	Merck[b]
N,*N*,*N*'*N*'Tetramethyl ethylene diamide (TEMED)	Accelerator	$C_6H_{16}N_2$	Molecular weight: 116.2 liquid, yellow	Merck[b]
Aluminum foil	Alumina source	Al	Foil	Merck[b]
Silica sol	Silica source	$[SiO_x(OH)_{4-2x}]_n$	Solution (27 wt%)	Merck[b]
Sodium hydroxide	Sodium source	NaOH	Solid white plate	Merck[b]

a- Fibrona, 215 M. Shirazi Street, Tehran, Iran.
b- E. Merck, D6100 Darmstadt, Germany.

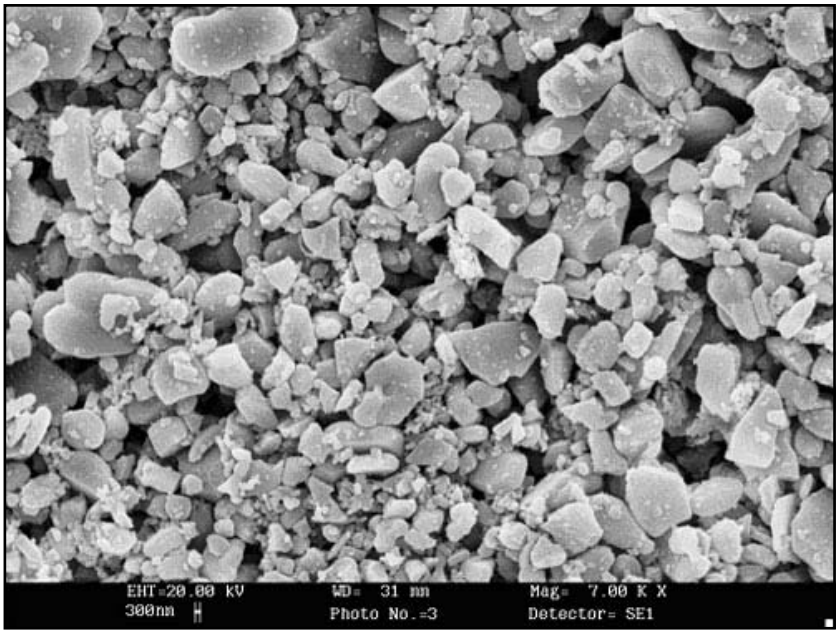

Figure 1. α -Alumina powder used in the synthesis of supports

Preparation of supports

Supports (12mm outer diameter and 7.5 cm length) were prepared by the gel-casting process. The flow sheet is illustrated in Figure 2 [12]. Appropriate amounts of monomers (5 weight percent based on the dried ceramic powder) were dissolved in demonized water to make the pre-mix solutions. Ceramic suspensions were then prepared by dis-persing the required volume fraction of support alumina powder (35 volume percent) to a pre-mix solution. Suspensions were mechanically stirred for the required time. The gelled parts were demoulded and dried (by a liquid desiccant drying method [13]), and then sintered at 1400 $^{\circ}$C for 5h.

Synthesis of sodalite top-layers

Sodalite seeds synthesis

The synthesis solution was prepared by mixing aluminate and silicate solutions. The aluminate solution was prepared by dissolving 10g sodium hydroxide in 39.75 ml of deionized water, then adding 0.25g of aluminum foil to the caustic solution. The silicate solution was prepared by mixing 8.52g sodium hydroxide, 5.15 ml silica sol and 39.75 ml deionized water. The aluminate solution, preheated to 60 $^{\circ}$C, was added to silicate solution by stirring. In order to produce a clear, homogeneous solution, the resulting mixture was stirred vigorously for 15 min. The molar ratio of this mixture solution was $5SiO_2$:Al_2O_3:$50Na_2O$:$1000H_2O$. The solution was poured into the Teflon holder of a stainless steel autoclave and heated at 363K for 6h. The synthesized sodalite zeolite seeds were washed several times with deionized water, and then air dried at 373K for 3h.

Support seeding

Porous supports were cleaned with deionized water in an ultrasonic cleaner for 5 min to remove the loose particles. Before coating the seeds or hydrothermal synthesis, the cleaned supports were held in air at 673K for 3h. The colloidal suspensions were prepared by dispersing 7g sodalite zeolite seeds in 1000 ml deionized water with ultrasonic treatment. The seeding layer was coated on the outer surface of the supports by a vacuum seeding method using a water pump, which

was used to create a pressure difference between the two sides of the supports wall. The coating pressure difference was monitored by a pressure gauge. The vacuum seeding was operated under the pressure difference 0.15 bar for 60, 120, 180 and 240 s. After vacuum seeding, the seeded supports were air dried at 373K for 3h.

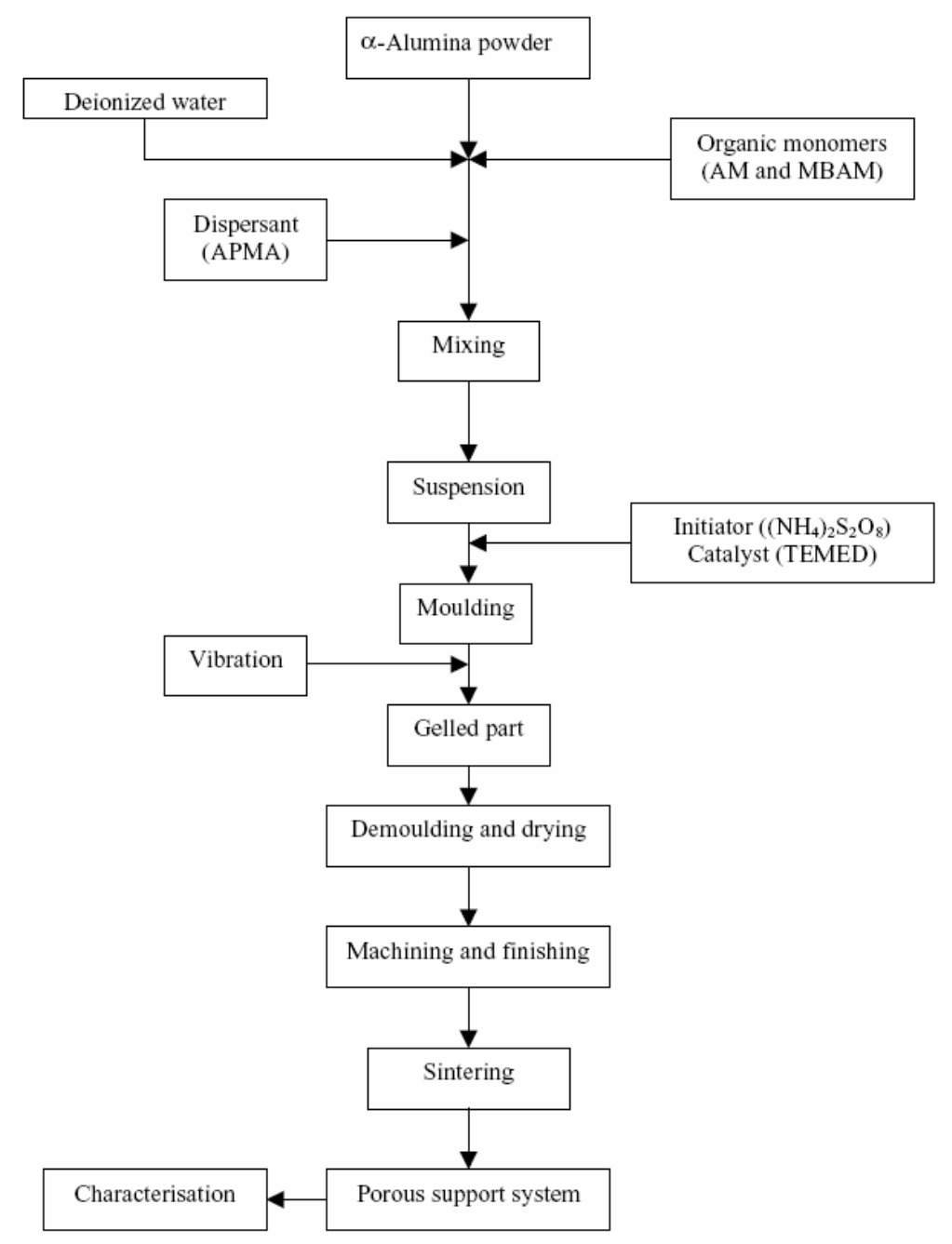

Figure 2. The preparation process of alumina porous support systems by water-based gel-casting method[12]

Sodalite top-layer secondary growth

The seeded support was placed vertically into the Teflon holder of a stainless steel autoclave to avoid any precipitation of sodalite zeolite crystals onto the support during the membrane synthesis. The synthesis solution prepared as mentioned in the "sodalite seeds synthesis" section was carefully poured into the autoclave without hitting the support, and the autoclave was then sealed. The crystallization was carried out in an air-circulated oven at 363 K for three stages (reaction time 6 h for each stage). The synthesized sodalite membrane was washed several times with deionized water, and then air dried at 373K for 3h.

Characterization

The porosity of the supports was measured with mercury porousimetery (Pascal-440, thermo finnigan, Italy, 1.8-7500 nm). The crystalline structure of the synthesized seeds and membranes was determined by X-ray diffraction (XRD) patterns. XRD was carried out on a TW3710 Philips X'Pert dif-fractometer using CuKα(λ=1.54 Å) radiation operating at 40kV and 50mA. Morphology and thickness of the synthesized sodalite membranes were examined by a scanning electron microscope (SEM, LEO 440I, 3×10^5, LEO, UK).

Single gas permeation measurement was carried out to evaluate the quality and performance of the membranes. The synthesized sodalite membranes were sealed in a permeation module with the zeolite membrane facing the high-pressure side. Measurements of H_2 and N_2 permeation were made at a temperature of 283 K and at pressure differences up to 0.6 MPa. Permeance was measured using the stainless steel permeator shown schematically in Fig. 3. Both annular ends between the membrane tube and the permeator wall were sealed with moulded RTV silicone gasket rings. All gases were introduced into the permeator by a calibrated multi-channel mass-flow controller. Feed gas flowed along the outside of the membrane and the permeated gases were measured on the inner side of the membrane at a temperature of 283 K and pressure 1 bar. Pressure differences across the membrane were obtained by varying the pressure on the upstream side and keeping the pressure constant downstream at 1 bar. Pressure in the shell side of the membrane module was monitored via a pressure gauge. The permselectivity of H_2/N_2 was defined as the permeance ratio of H_2 and N_2.

Result and Discussion

Porous support systems

Figure 4 shows the SEM micrograph of the prepared support. This indicates that the surface of the support is defect free. Figure 5 shows that the pore size of the prepared supports are 100-800nm with an average pore size of 570 nm. The open porosity of these supports was determined to be more than 47% by mercury porosimetry and Archimedes methods. The obtained results confirm that these supports are suitable for manufacturing zeolite-composite membranes.

Synthesized sodalite seeds

The synthesized sodalite seeds were characterized by XRD and SEM. Fig.6 shows the XRD pattern of the synthesized sodalite zeolite. It can be seen that the diffraction pattern of the synthesized zeolite confirms the synthesis of sodalite zeolite in comparson with the reference sodalite zeolite diffraction pattern. As shown in Fig.7, the SEM micrograph indicates the morphology of the synthesized sodalite zeolite seeds as spherical particles.

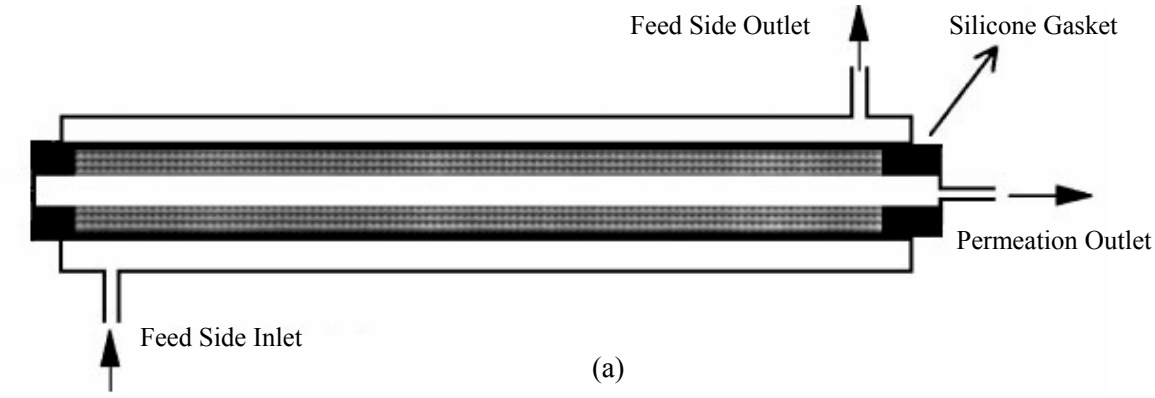

(a)

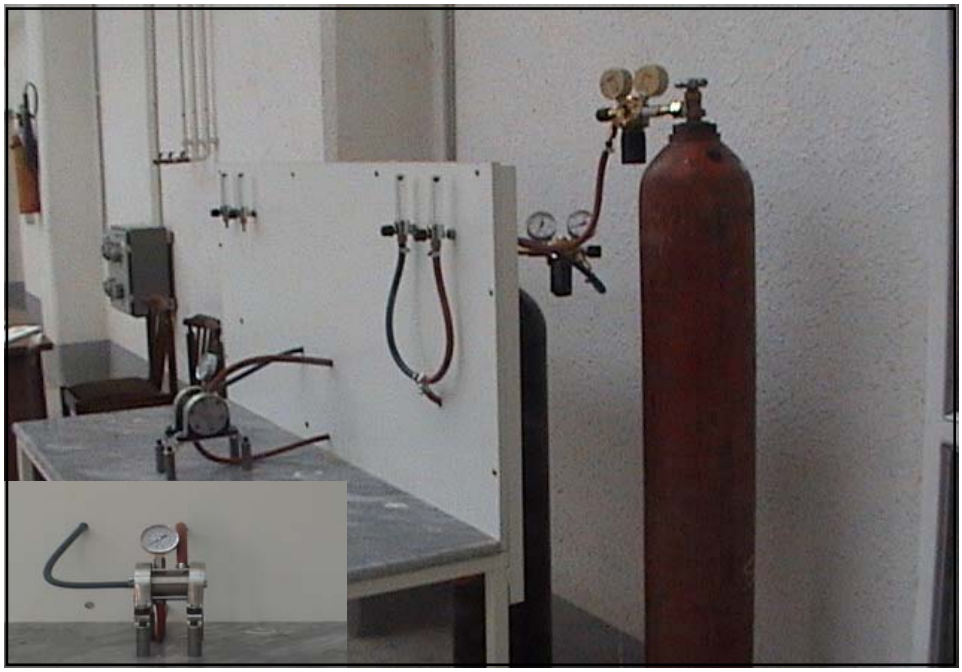

(b)

Figure 3. a) Schematic (diagram) of a tubular permeator, b) Stainless steel permeator set-up

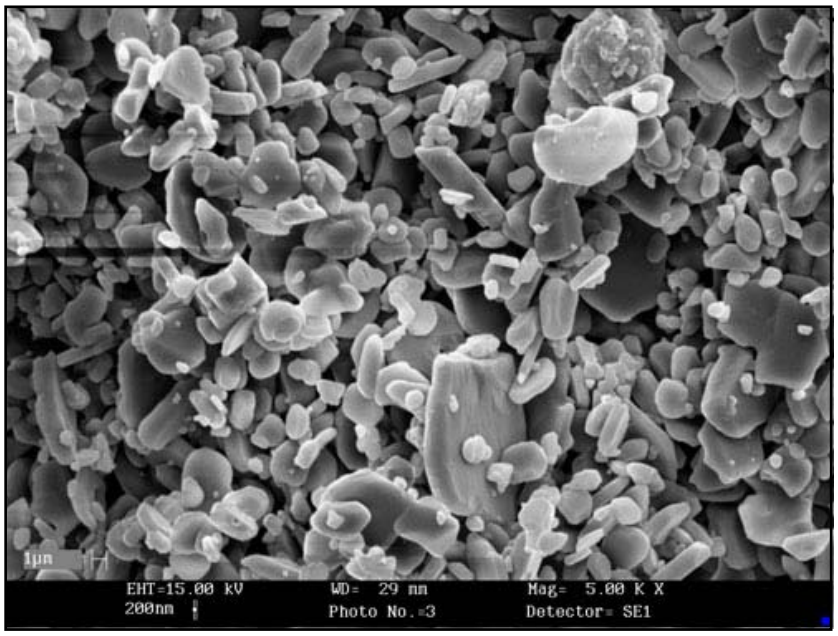

Top view

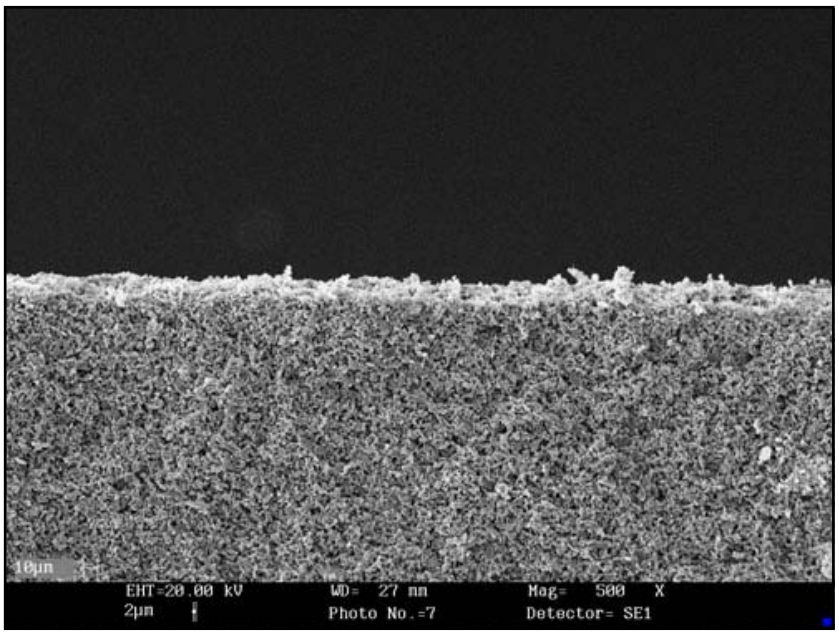

Cross-section

Figure 4. SEM micrograph of the prepared support

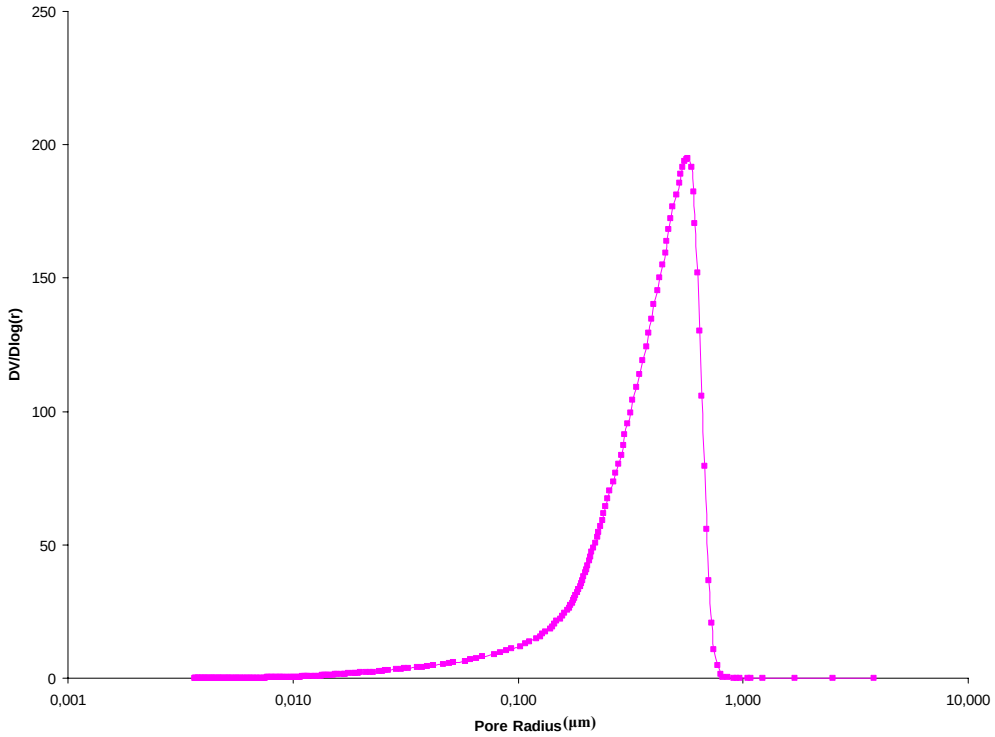

Figure 5. Mercury porosimetry results on the supports pore size distribution

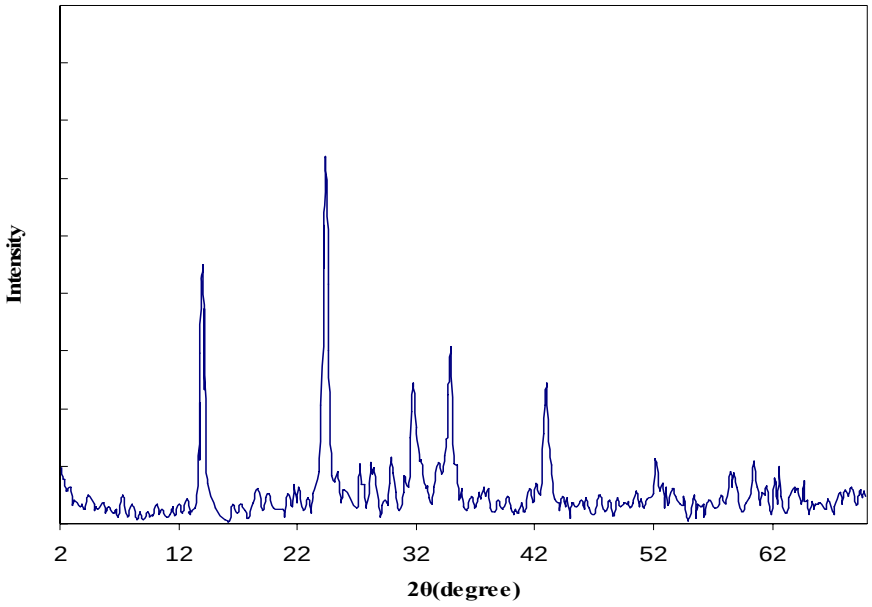

Figure 6. XRD pattern of the synthesized sodalite zeolite seeds

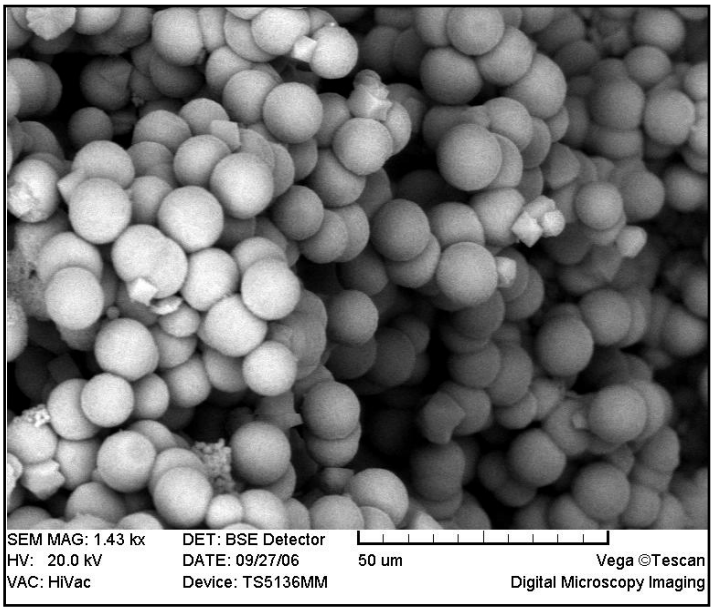

Figure 7. SEM micrograph of the synthesized sodalite zeolite seeds

Synthesized sodalite membranes

In order to form a thin and uniform sodalite zeolite membrane on the support, the nucleation seeds should be uniform in size and larger than the pore size of the support.

The XRD patterns of the manufactured sodalite membranes with different seeding times were presented in Fig.8. It is found that the thin films formed on the supports surface are sodalite zeolite and the observed extra picks can be due to the α -Al_2O_3 support system. Fig.9 shows the SEM micrographs of the prepared membranes top-layers. As can be seen, after three-stage synthesis (reaction time 6 h for each stage), the surface of alumina supports are completely covered with a uniform layer of randomly oriented sodalite crystals.

Also, the cross section micrographs of the sodalite membranes are shown in Fig. 10. It is observed that by increasing the seeding time, sodalite membranes thickness increases and reaches to a maximum value at 180 s. As shown in Fig.11, the seeding time has a great effect on the microstructure of the prepared sodalite membranes, so that a thick and low-dense top-layer was formed in the membranes manufactured with a seeding time of 180s. Further increase in seeding time causes dense top-layers to form with the same thickness.

The effect of seeding time on zeolite membranes thickness is not well-established. But, as mentioned in the literature, at low seeding time the support surface was not completely covered by a continuous seeding layer [14]. However, at seeding time in the range of 60-90s, a uniform seeding layer and finally a dense and continuous zeolite membrane layer was formed on the support surface. By increasing the seeding time, the support surface was covered by zeolite seeds with a multilayer structure, and zeolite membrane layers were constructed with high thickness and porosity. By further increasing the seeding time (>180s), (although the applied vacumn was not able to increase the thickness of the seeded layers), relatively dense layers of zeolite seeds with a fixed thickness were formed on the support surface during the long seeding time. A similar structure was observed in the final zeolite membrane layers.

However, a permeation test was carried out in order to attain a more exact investigation of the seeding time effect.

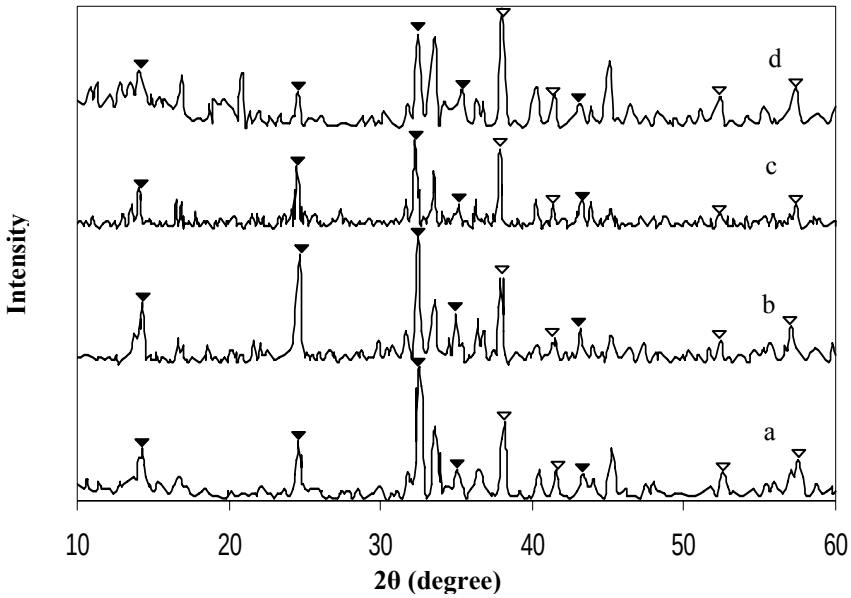

Figure 8. XRD patterns of the synthesized membranes with seeding time: a) 60s, b) 120s, c) 180s, d) 240s; (▽) α-Al_2O_3, (▼) Sodalite zeolite.

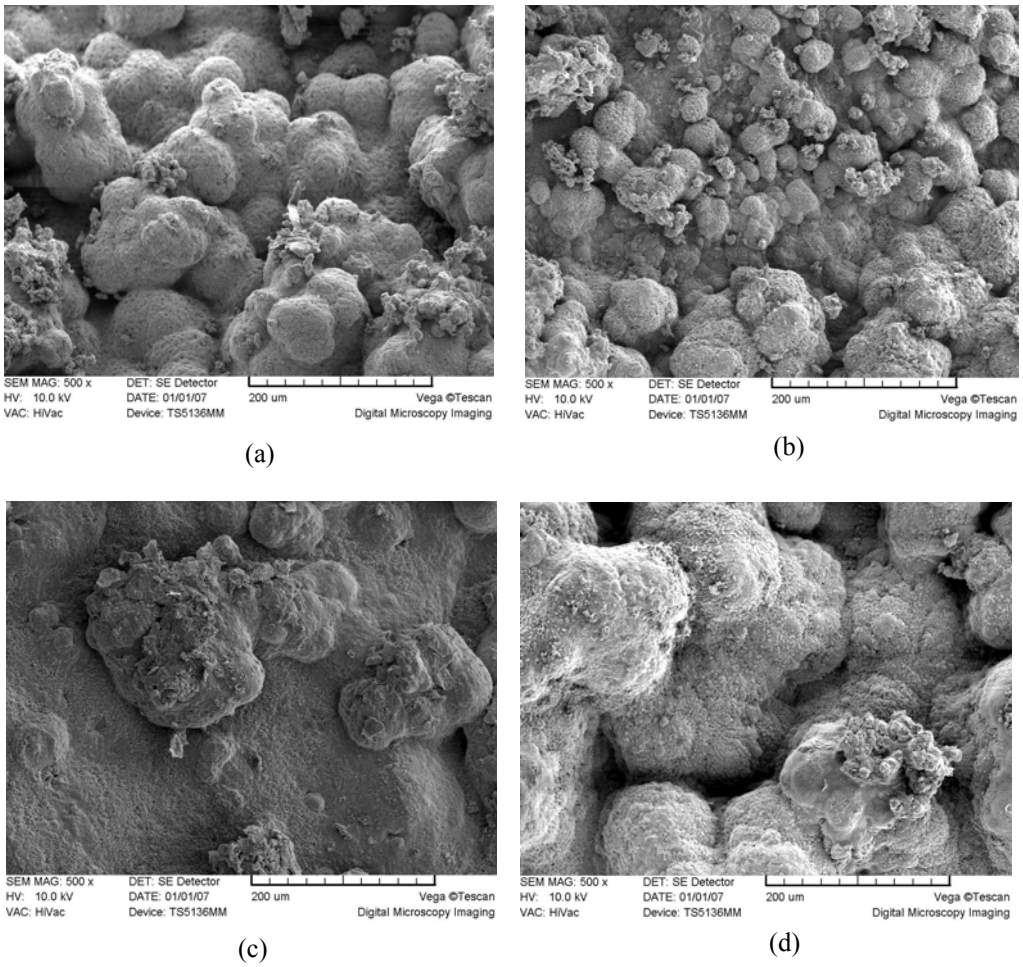

Figure 9. Top-view SEM micrographs of the prepared membranes top-layers with seeding time: a) 60 s, b) 120 s, c) 180 s, d) 240 s.

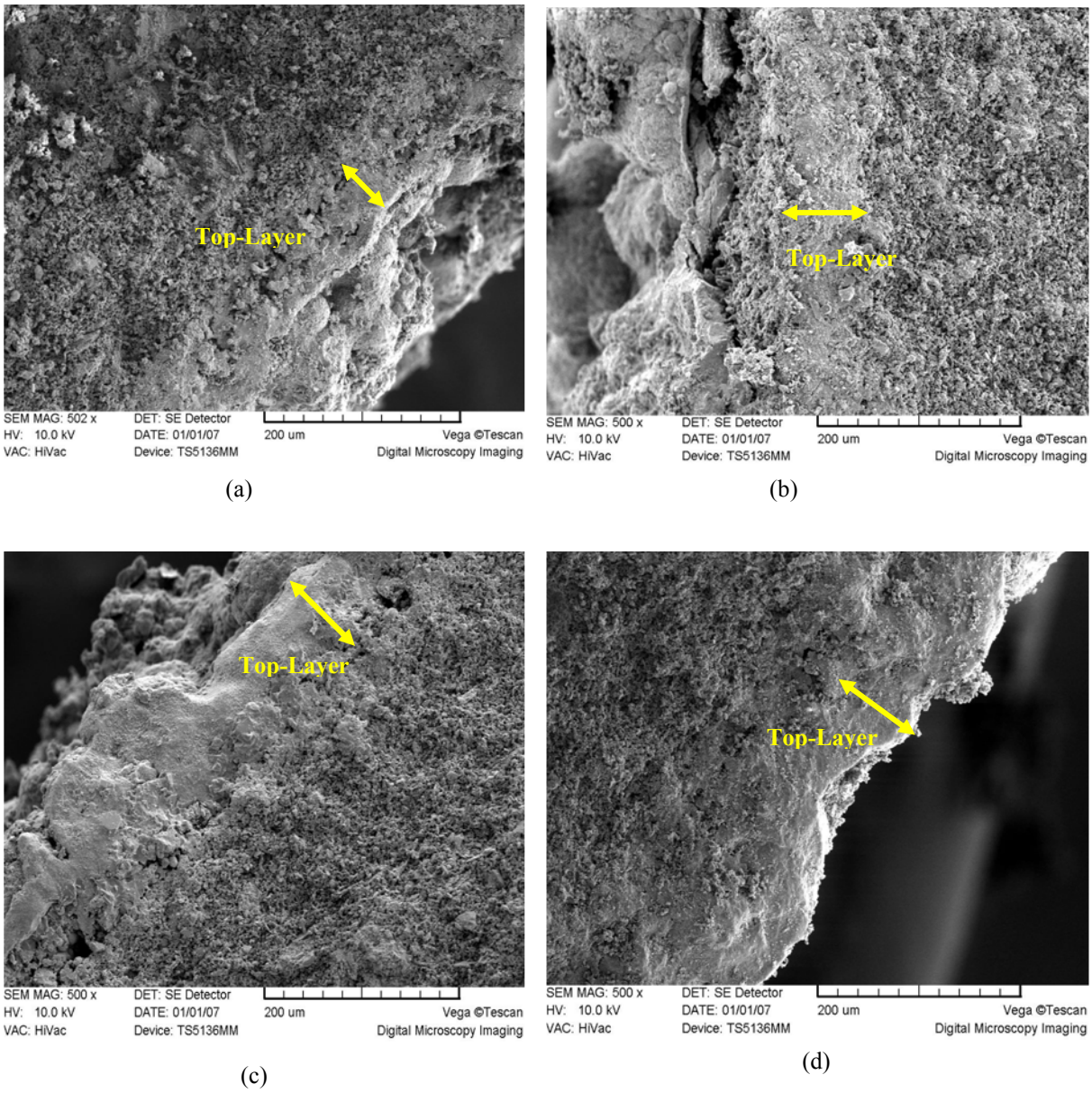

Figure 10. Cross section SEM micrographs of the prepared membranes top-layers with seeding time: a) 60 s, b) 120 s, c) 180 s, d) 240 s.

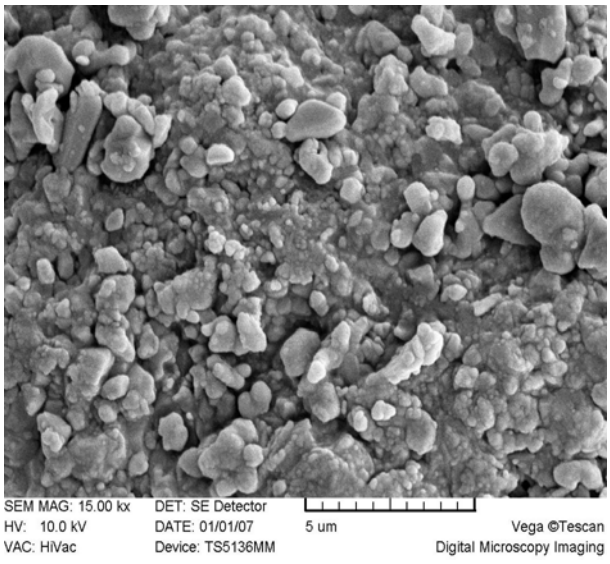

(a)

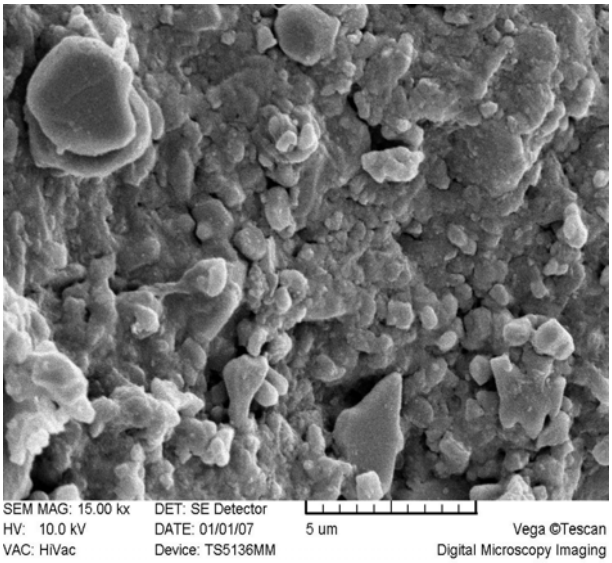

(b)

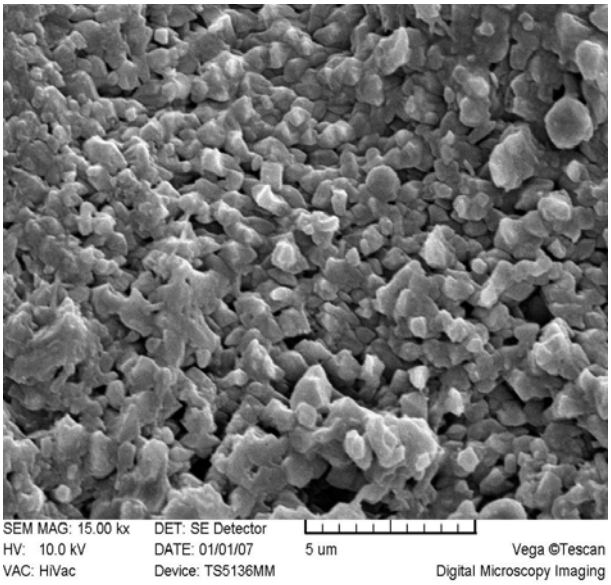

(c)

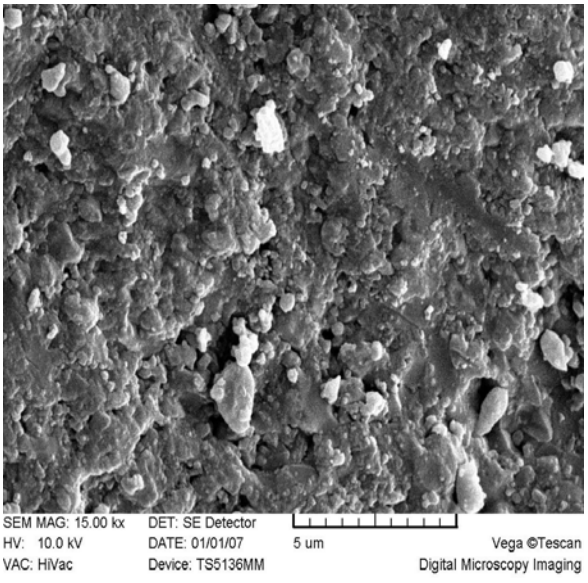

(d)

Figure 11. Cross section microstructure of the prepared membranes top-layers with seeding time: a) 60 s, b) 120 s, c) 180 s, d) 240 s.

Single gas permeation studies

Gas permeation properties of the synthesized sodalite membranes with the reaction time 6 h after a three-stage synthesis were measured under different pressure differences. Fig. 12 shows the permeance of single gases (H_2 and N_2) as a function of pressure difference at a temperature of 283K for the manufactured membranes with different seeding times. The permeance of H_2 and N_2 shows little dependence on the pressure difference. The higher permeation of H_2 could be observed compared with that of N_2 due to the kinetic diameter of gases (N_2=3.64 A° and H_2=2.89 A° [11]).

The obtained results from the literature [15] showed that the more technologically interesting hydrogen loadings in sodalite are found only to be achieved under extremely low temperature (<200 K) and/or extremely high pressure (>100 bars) conditions. Therefore, the adsorption-diffusion mechanism in sodalite membranes can not be applied in ambient temperature and low pressures. In other words, the single gas permeation flux in ambient conditions is due to the permeability of the inter-crystalline pores. Finally it can be concluded that the permeation of single gases through the sodalite membranes at ambient conditions can be attributed to the transition flow mechanism not to molecular sieve structures.

In the transition flow mechanism both viscous (or Poiseuille) flow and Knudsen diffusion mechanisms have influence:

Viscous or Poiseuille flow mechanism flux:

$$J_v = -\frac{r^2}{8\eta}.\frac{\overline{P}}{RT}.\frac{\Delta P}{\Delta z} = \frac{\overline{P}.\Delta P}{R_p} \qquad (1)$$

Knudsen diffusion mechanism flux:

$$J_k = -\frac{2}{3}\bar{v}r\frac{1}{RT}.\frac{\Delta P}{\Delta z} = \frac{\Delta P}{R_K} \qquad (2)$$

where ΔP is the pressure difference across the membrane, Δz is the membrane thickness, r is the mean pore radius, R is the gas constant, T is the absolute temperature, η is the gas viscosity and $\bar{v}$ is the average velocity of (the) gas molecules.

Therefore, the relation for the permeance of gases in the manufactured nanostructure sodalite membranes can be obtained as follows [16, 17]:

$$Permeance\left(\frac{mol}{m^2 \cdot s \cdot Pa}\right) = \frac{J\left(\frac{mol}{m^2.s}\right)}{\Delta P(Pa)} = \frac{1}{R_k} + \frac{\overline{P}}{R_p} \qquad (3)$$

which R_k is the Knudsen resistance and R_p is the Poiseuille resistance defined independent of the pressure conditions. Thus, the values of the gas permeance are a linear function of the arithmetic mean gas pressure in permeator ($\overline{P}$) as shown in Fig. 13. Also, the permselectivity of the H_2/N_2 binary gas mixture was presented in Fig. 14 as a function of the pressure difference. The obtained results show an ideal selectivity of about 2.1-2.5 which confirms transition flow mechanism (both viscous flow and Knudsen diffusion) in gas separation processes by the manufactured membranes.

As shown in Figs. 12 and 13, the permeance of the prepared sodalite membranes increases by increasing seeding time and shows a maximum point at 180 s, but, the seeding time does not have a significant effect on the selectivity (see Fig. 14). A high significant effect of the seeding time on the membranes permeance can be due to the top-layers microstructure formed at different seeding times. This behavior was confirmed by the SEM micrographs of the manufactured sodalite membranes which showed a porous and low dense layer at seeding time 180 s with uniform surface (see Figs. 9 and 11).

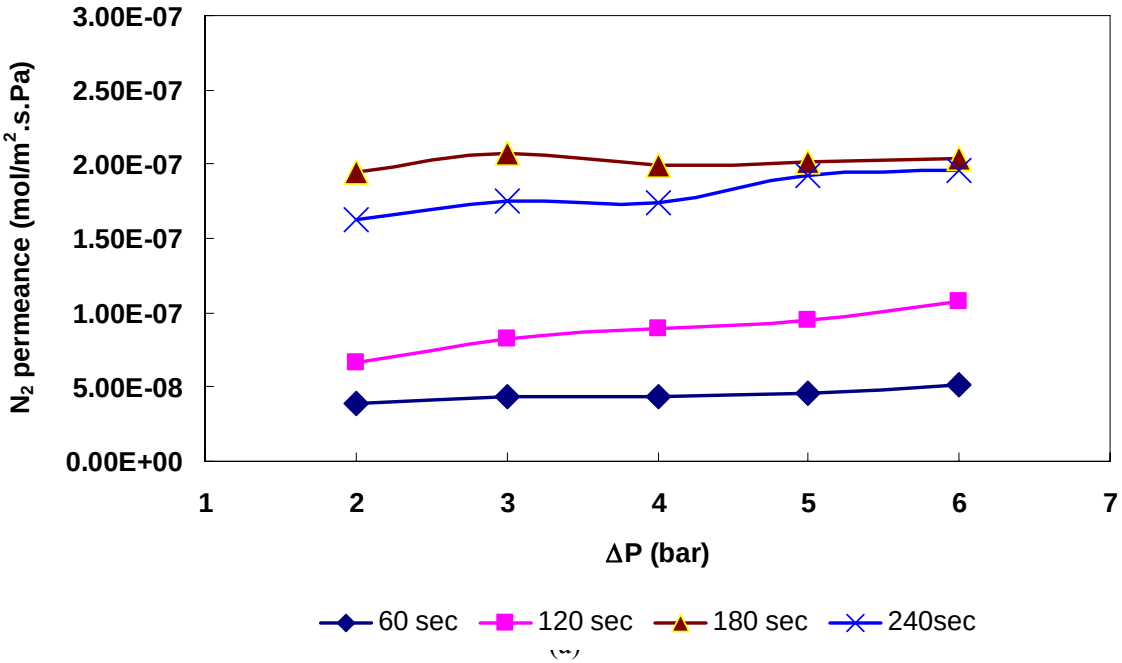

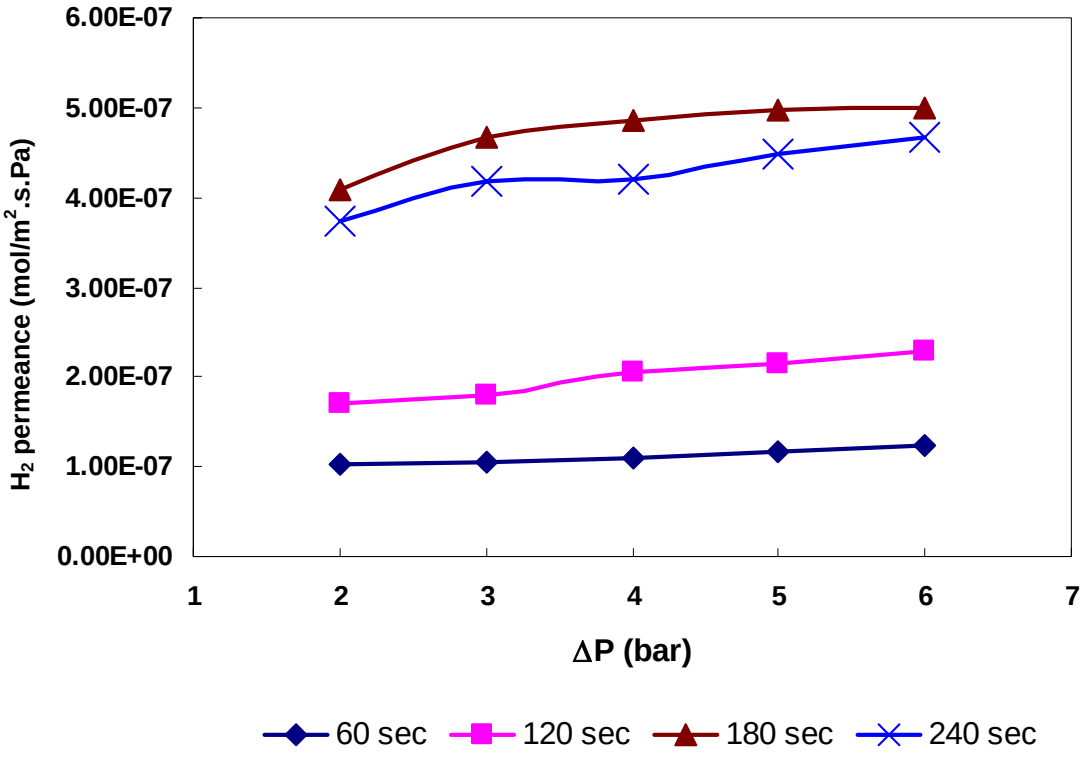

(b)

Figure 12. Permeance of the sodalite zeolite membranes at 283 °K for a) N_2 and b) H_2 as a function of pressure difference at different seeding times

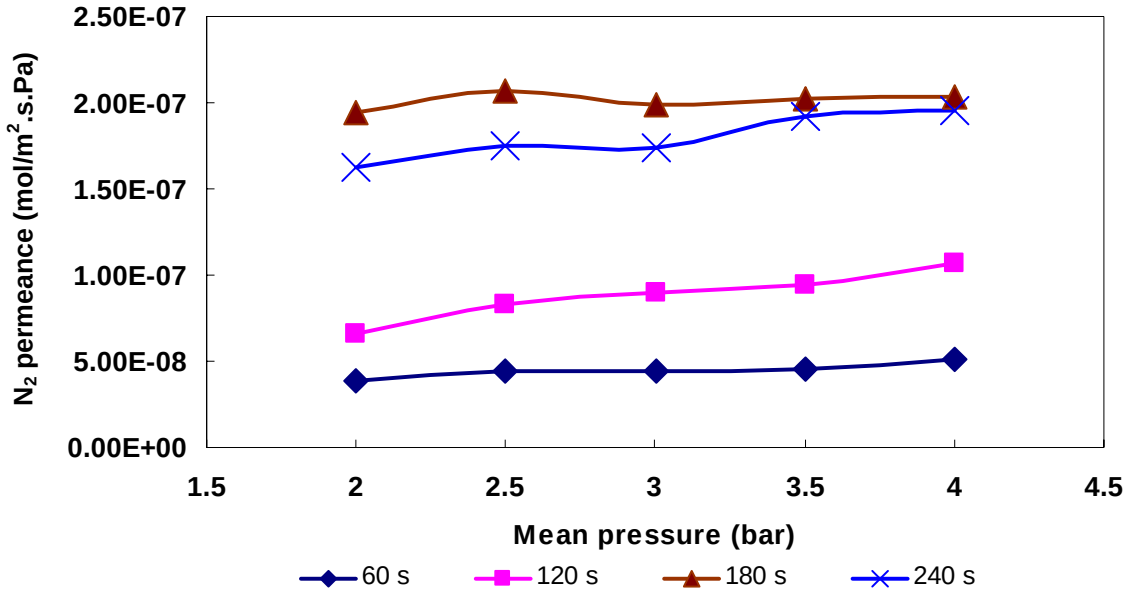

(a)

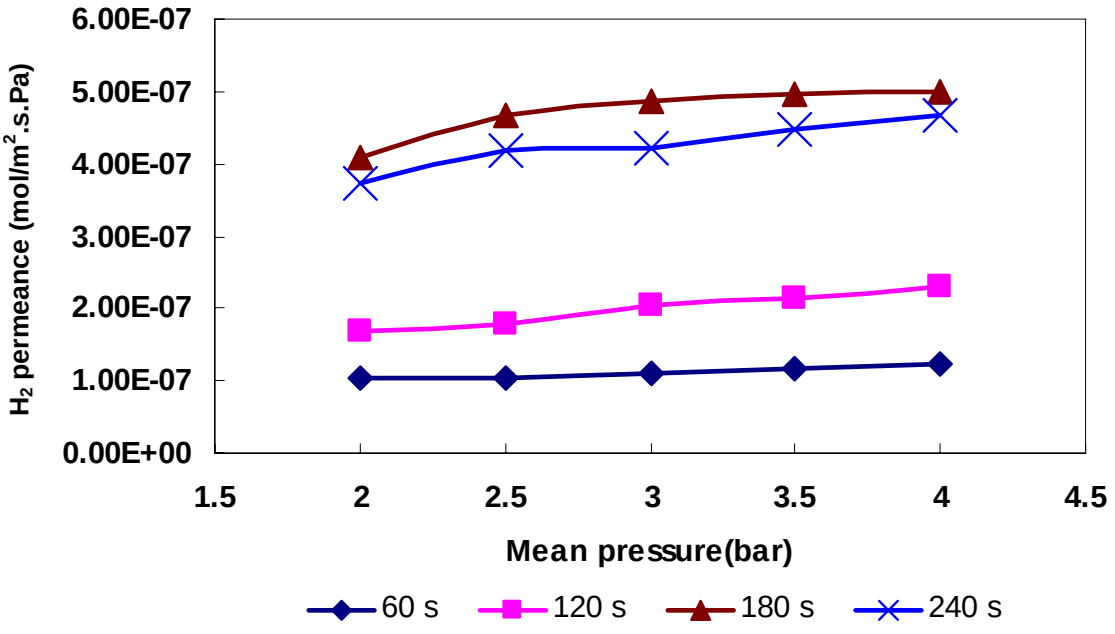

(b)

Figure 13. Permeance of the sodalite zeolite membranes at 283 °K for a) N_2 and b) H_2 as a function of mean pressure at different seeding times

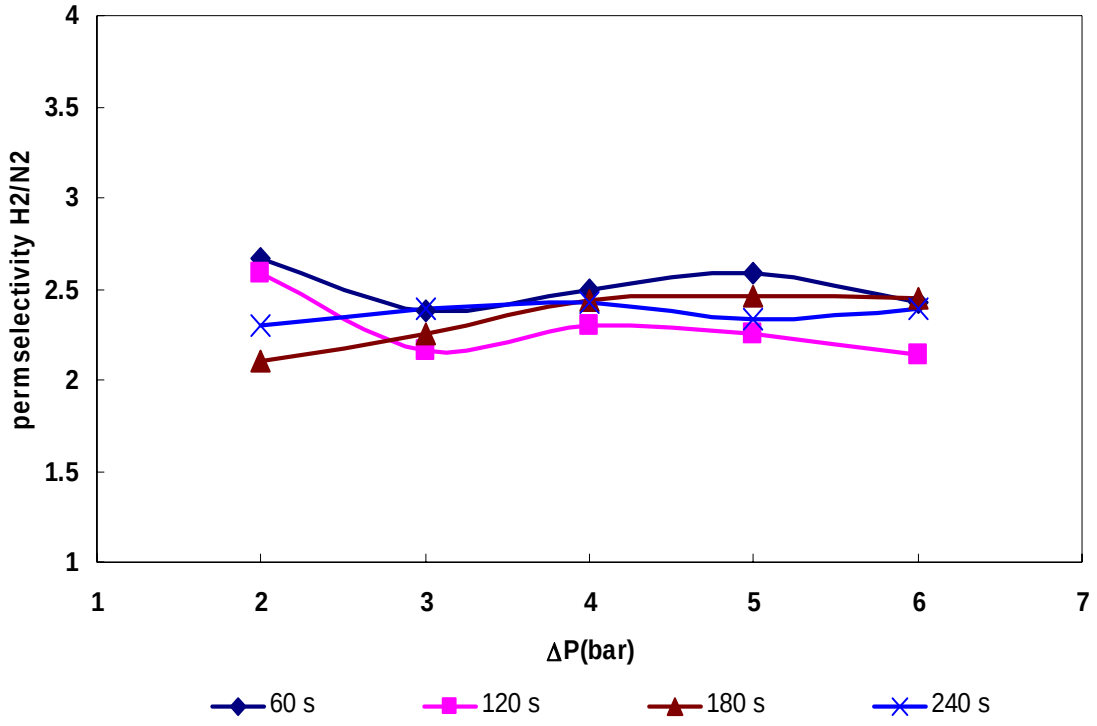

Figure 14. Permselectivity of the sodalite zeolite membranes at 283 °K for H_2/N_2 binary mixture as a function of (mean) pressure difference at different seeding times

As mentioned earlier, by increasing the seeding time, the support surface was covered by zeolite seeds with a multilayer structure, and zeolite membrane layers were constructed with high thickness and porosity. Therefore, increasing the membrane permeance at high seeding times can be due to the formation of high intercrystal porous structures. Further increasing seeding time results in relatively dense zeolite membrane layers with a fixed thickness. This trend confirmed a relative decrease of membrane permeance by further increasing the seeding time.

Conclusions

The obtained results in this work are presented as follows:

1. Nanostructure sodalite membranes with uniform structures were successfully synthesized on α-Al_2O_3 tubular supports from a synthesis mixture via secondary growth.
2. By increasing seeding time, the thickness of the prepared sodalite top-layers increases and tends to plateau. Further increasing the seeding time causes dense top-layers with the same thickness to form.
3. Single gas permeation properties of the nanostructure sodalite membranes were studied. The obtained results showed that in the gas permeation through the manufactured sodalite membranes, both viscose flow and Knudsen diffusion mechanisms have influence (i.e. transition flow mechanism).
4. The gas permeation results showed that by increasing seeding time, permeance of the sodalite membranes manufactured via the secondary growth method increases dramatically to reach a maximum point at

180s. Further increasing seeding time results in relatively low permeable membranes. This behavior was verified by microstructure micrographs of the sodalite membranes.

Acknowledgments

The Authors wish to thank Sahand University of Technology (SUT) and Tabriz Refinery for the financial support of this work. We also thank the co-workers and technical staff in the Chemical Engineering Department, the Research Center for Polymeric Materials and the Nanostructure Materials Research Center of SUT for their help during various stages of this work.

References

1. Sathupunya, M., Gulari, E., and Wonghasemjit, S., ANA and GIS zeolite synthesis directly from alumatrane and silatrane by sol-gel process and microwave techniques, *J. Eur. Ceram. Soc.*, **22**, 2305 (2002).
2. Sathupunya, M., Gulari, E., and Wonghasemjit, S., Na-A (LTA) zeolite synthesis directly from alumatrane and silatrane by sol-gel microwave techniques, *J. Eur. Ceram. Soc.*, **23**, 1293 (2003).
3. Chen, L., and Deem, M.W., Strategies for high throughput, templated zeolite synthesis, *Mol. Phys.***, 100**, 2175 (2002).
4. Pak, A., and Mohammadi, T., Zeolite NaA membranes synthesis, *Desalination*, **200**, 68 (2006).
5. Xu, X., Yang, W., Liu, J., and Lin, L., Synthesis of NaA zeolite membranes from clear solution, *Micro and Mesoporous Materials***, 43,** 299 (2001).
6. Kazemi Moghadam, M., Pak, A., and Mohammadi, T., Dehydration of water/1-1-dimethylhydrazine mixtures by zeolite membranes, *Micro and Mesoporous Materials***, 70**, 127 (2004).
7. Buhl, J.C., Gesing, Th.M., Kerkamm, I., and Gurris, Ch., Synthesis and crystal structure of cyanate sodalite $Na_8(OCN)_2[Al_6Si_6O_{24}]$, *Micro and Mesoporous Materials***, 65,** 145 (2003).
8. Julbe, A., Motuzas, J., Cazevielle, F., Volle, G., and Guizard, C.**,** Synthesis of sodalite/α-Al2O3 composite membranes by microwave heating, *Separation and Purification Technology*, **32,** 139 (2003).
9. Manna, G.L., Barone, G., Varga, Z., and Duca, D., Theoretical evaluation of structures and energetics involve in the hydrogenation of hydrocarbons on palladium surfaces, *J. of Molecular Structure*, **548,** 173 (2001).
10. Lee, S., Son, Y. H., Julbe, A., and Choy, J. H., Vacuum seeding and secondary growth route to sodalite membrane, *Thin Solid Films***, 495,** 92 (2006).
11. Xu, X., Baoa, Y., Song, C., Yang, W., Liua, J., and Lina, L., Synthesis, characterization and single gas permeation properties of NaA zeolite membrane, *J. Memb. Sci.*, **249**, 51 (2005).
12. Bayati, B., and Babaluo, A.A., Manufacturing porous supports of ceramic membranes and debinding behavior in gel-casting method, *Proceeding of 11nd chemical engineering congress*, Tarbiat Modares University, Tehran, Iran, Nov. 28-30, 2006.
13. Barati, A., Kokabi, M., and Famili, M.H.N., A novel method in drying gelcast ceramic articles, *Ceram. Int*., **29,** 199 (2003).
14. Huang, A., Lin, Y.S., and Yang, W., Synthesis and properties of A-type zeolite membranes by secondary growth method with vacuum seeding, *J. Memb. Sci*., **245**, 41 (2004).
15. Annemieke, W.C., Bromley, S.T., Wojdel, J.C., and Jansen, J.C., Adsorption isotherms of H_2 in microporous materials with the SOD structure: A grand canonical Monte Carlo study, *Micropor. and Mesopor. Mat.*, **87**, 235 (2006)
16. Uchytil, P., and Broz, Z., Gas separation in ceramic membranes Part I. Theory and testing of ceramic membranes, *J. Memb. Sci.*, **97,** 139 (1994).
17. Uchytil, P., and Broz, Z., Gas separation in ceramic membranes Part II. Modeling of gas permeation through ceramic membrane with one supported layer, *J. Memb. Sci.*, **97,** 145 (1994).